ChemComm

# Quinoxaline radical-bridged transition metal complexes with very strong antiferromagnetic coupling



| | |
|---|---|
| Journal: | *ChemComm* |
| Manuscript ID | CC-COM-05-2020-003713.R1 |
| Article Type: | Communication |
| | |

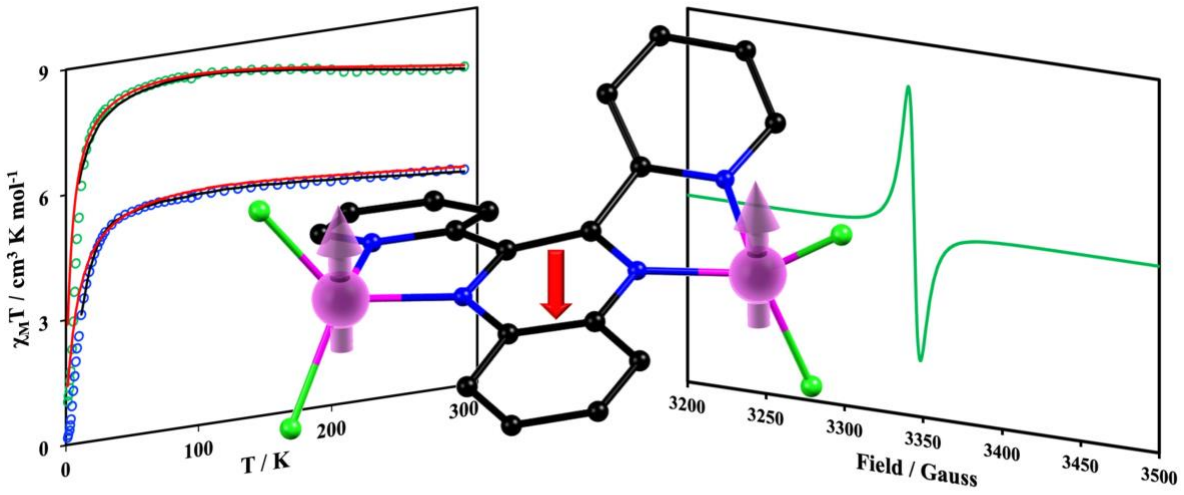


Synthesis, magnetic studies and, theoretical calculations of a new family of transition metal complexes bridged by a quinoxaline-based radical.

COMMUNICATION

# Quinoxaline radical-bridged transition metal complexes with very strong antiferromagnetic coupling

Received 00th January 20xx,
Accepted 00th January 20xx

DOI: 10.1039/x0xx00000x

Dimitris I. Alexandropoulos, Kuduva R. Vignesh, Haomiao Xie, and Kim R. Dunbar*

**A new family of radical-bridged compounds, $(Cp^*_2Co)[M_2Cl_4(dpq)]$ (M = Fe (1), Co (2), Zn(3)), (dpq = 2,3-di(2-pyridyl)-quinoxaline) is reported. Magnetic studies, DFT and *ab initio* calculations reveal strong antiferromagnetic metal-radical interactions with coupling constants of $J$ = -213.1 and -218.8 $cm^{-1}$ for 1 and 2, respectively.**

Molecular magnetic materials[1] are of paramount interest for many technological applications including high density data storage,[2] molecular electronic devices,[3] and quantum computation.[4] The syntheses of these materials often rely on self-assembly reactions between paramagnetic metal ions and organic bridging ligands which offer the advantages of thermodynamic stability, solubility, and crystallinity. The success of this approach notwithstanding, the presence of closed-cell bridging ligands often limits the properties and dynamics of magnetic materials, leading to competing magnetic interactions, moderate-to-weak magnetic coupling, and low-lying excited states, among others. A successful strategy to overcome these obstacles is to use organic radicals as bridging ligands between metal spin centers which leads to stronger direct magnetic coupling as compared to the indirect superexchange interactions observed in the case of diamagnetic linkers.[5] Indeed, a number of interesting radical bridged transition metal and lanthanide complexes have been reported to date, including the $[K(18\text{-crown-}6)(THF)_2][\{[(Me_3Si)_2N]_2(THF)Ln\}_2(\mu\text{-}\eta^2\text{:}\eta^2\text{-}N_2)]$ compound that exhibits magnetic hysteresis up to 14 K[6] as well as the complex $[(TPyA)_2Fe_2(^{NPh}L)](SO_3CF_3)$ (TPyA = tris(2-pyridylmethyl)- amine, $^{NPh}LH_2$ = N,N′,N′′,N′′′-tetraphenyl- 2,5-diamino-1,4-diiminobenzoquinone)[7] which exhibits a coupling constant of 900 $cm^{-1}$. In general, however, radical bridged metal complexes have been far less studied and in many ways are in their infancy than examples bridged by innocent closed-shell ligands.

Research in our group has focused on the design of metal complexes bearing the radical forms of tetrazine-based ligands, including 3,6-bis(pyridyl)-1,2,4,5-tetrazine (bptz) and 3,6-bis(pyrimidyl)-1,2,4,5-tetrazine (bmtz). The implementation of these ligands in both 3d and 4f metal chemistry has afforded structurally interesting compounds including bimetallic species as well as supramolecular architectures.[8] Recently, we turned our attention to other, relatively unexplored, non-innocent ligands that can undergo redox chemistry to stabilize radical isomers. Taking into account its bridging capabilities,[9] together with its reversible electrochemical reduction at -1.95 V versus $Fc/Fc^+$ in MeCN (Figure S2), we investigated reduced bimetallic transition metal complexes of the 2,3-di(2-pyridyl)-quinoxaline (dpq). Herein, we report the syntheses, structures and magnetic properties of three new bimetallic complexes, *viz*., $(Cp^*_2Co)[M_2Cl_4(dpq)]$ (M = Fe (**1**), Co (**2**), and Zn(**3**)). To the best of our knowledge, these compounds are the first examples in which the dpq ligand is in its radical anion form.

Compounds **1-3** were prepared by the reaction of anhydrous $MCl_2$ (M = Fe, Co, Zn) and dpq in a 2:1 molar ration in the presence of 1 equivalent of reducing agent $Cp^*_2Co$ in MeCN. Layering of the resulting solutions with $Et_2O$ afforded crystals suitable for X-ray analyses in high yields of 55-75%. Complexes **1-3** are isostructural, thus only the structure of **1** will be described as a representative example. The molecular structure of the anion of **1** (Figure 1) consists of two crystallographically inequivalent Fe atoms linked by a bridging dpq ligand. Each metal is four-coordinate with a distorted tetrahedral geometry. Two coordination sites are occupied by a chelating N-donor dpq ligand with the remaining two being filled by two terminal $Cl^-$ ions. The geometry[10] for Fe1 and Fe2 in **1** exhibits average dihedral angles of 76.5° and 77.0° which further supports the fact that each Fe is in a distorted tetrahedral geometry. Complexes **2** and **3** exhibit similar dihedral angles (77.9° for Co1/Co2, 78.3° for Zn1 and 78.2° for Zn2). The oxidation state of the Fe atoms is established as 2+ by charge balance

‡ *Department of Chemistry, Texas A&M University, College Station, Texas 77842-3012, United States. Email: dunbar@chem.tamu.edu*
Electronic Supplementary Information (ESI) available: Synthetic, Crystallographic, and Magnetic details. See DOI: 10.1039/x0xx00000x

considerations and bond valence sum (BVS)[11] calculations (SI). The dpq ligand is considerably distorted; the two pyridine rings are twisted by 28.9° and 25.6° (28.4° and 24.2° in **2**; 28.3° and 25.9° in **3**) with respect to the mean plane of the quinoxaline group, which is also distorted.

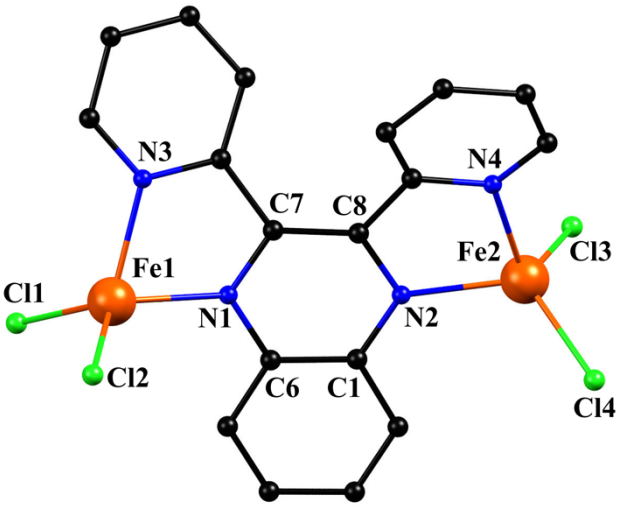


**Figure 1.** Labeled representation of **1**. Colors: $Fe^{II}$, orange; N, blue; C, black, Cl, green. Hydrogen atoms are omitted for the sake of clarity.

A close inspection of the quinoxaline C-C (C1-C6, C7-C8) and C-N (N1-C6, N1-C7, N2-C1, N2-C8) bond distances in **1-3** revealed average distances of 1.403(5) Å and 1.372(5) Å, respectively. These values deviate significantly from the reported values for the neutral dpd ligand (C-C: ~1.423(4) and C-N: ~1.344(4))[9a-c], reflecting the net decrease in C-C bond order and a net increase in C-N bond order. These parameters are indicative of the presence of an additional electron in the ligand molecular orbitals, which is further supported by the short M-$N_{pz}$ distances (M = Fe: 2.043(2), Co: 1.966(3), Zn: 2.022(4)) observed in **1-3**, consistent with a strong metal-ligand interaction. Finally, the solid-state X-band EPR spectrum of the Zn analogue **3** at 293 K, shown in Figure 2, features a single resonance centered on g = 2.0046, confirming the presence of the dpq radical.

Solid-state direct-current (*dc*) magnetic susceptibility ($\chi_M$) data on dried and analytically pure samples of **1** and **2** were collected in the 2-300 K range at an applied field of 0.1 T and are plotted as $\chi_M T$ vs. T in Figure 3. For **1**, the experimental $\chi_M T$ value (7.63 $cm^3$ K $mol^{-1}$) at 300 K is considerably higher that the theoretical value of 6.38 $cm^3$ K $mol^{-1}$ for two non-interacting high-spin, S = 2, $Fe^{II}$ ions and one S = 1/2 dpq radical (g = 2.0), due to spin-orbit coupling contributions.[12] Upon cooling, the $\chi_M T$ product increases gradually to a value of 8.41 $cm^3$ K $mol^{-1}$ at 75.0 K. Below this temperature $\chi_M T$ decreases sharply to a value of 1.03 $cm^3$ K $mol^{-1}$ at 2.0 K. The $\chi_M T$ value at 75 K is very close to that expected for an S = 7/2 ground state (8.35 $cm^3$ K $mol^{-1}$, g = 2.06), arising from strong antiferromagnetic metal-radical interactions, while the low temperature decrease can be attributed to zero-field splitting as well as antiferromagnetic inter- or intra-molecular metal-metal interactions.

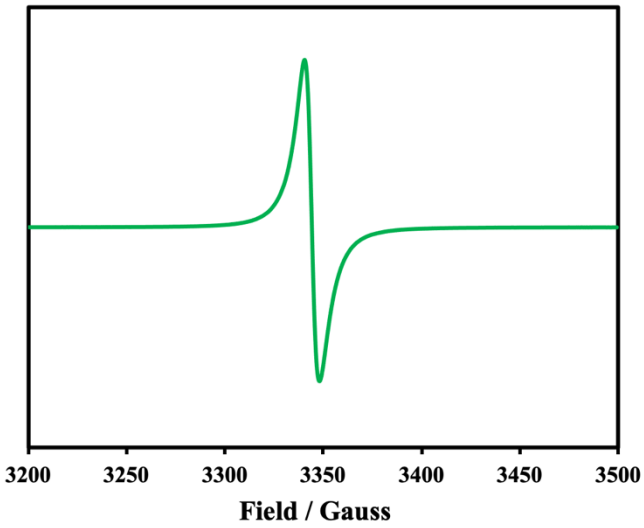


**Figure 2.** Solid-state X-band EPR spectrum of **3** at 293 K with microwave frequency 9.390 GHz.

Complex **2** exhibits similar behavior, with $\chi_M T$ slightly increasing from 5.19 $cm^3$ K $mol^{-1}$ at 300 K to a maximum of 5.48 $cm^3$ K $mol^{-1}$ at 75 K, and then sharply decreasing to 0.28 $cm^3$ K $mol^{-1}$ at 2.0 K. The 300 K value for **2** is higher than the spin-only (*g* = 2) value of 4.13 $cm^3$ K $mol^{-1}$ for two non-interacting high spin $Co^{II}$ ions (S = 3/2) and one dpq radical (S= 1/2), which reflects strong orbital angular momentum contributions. The shape of the curve indicates dominant antiferromagnetic exchange interactions between the $Co^{II}$ ions and the dpq radical corresponding to a ferrimagnetic *S* = 5/2 ground state for **2**. Also, the reduced magnetization data for **1** and **2** (Figures S4-S5) indicate significant *D* values for both complexes and/or population of low-lying excited states since the isofield lines do not superimpose onto a single master curve.

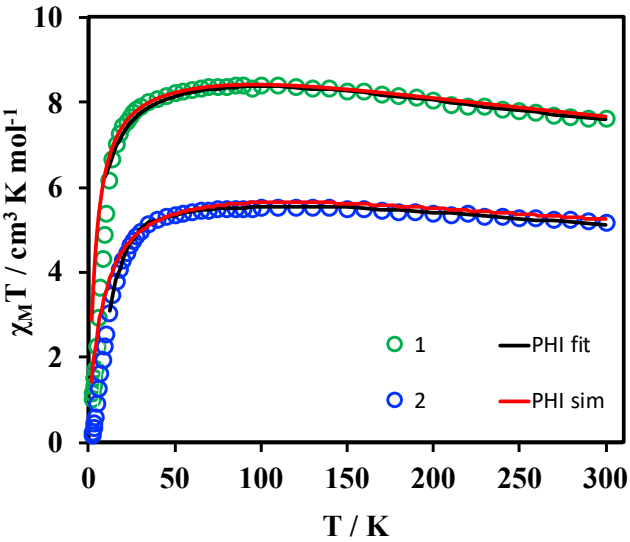


**Figure 3.** $\chi_M T$ vs. T plots for **1** and **2**. Black lines represent fit of the experimental data according to spin Hamiltonian described in the text. Red curves represent simulations based on DFT data.

To estimate the metal-radical magnetic exchange interactions in **1** and **2** the magnetic susceptibility data above 10 K were fit using the PHI program[13] according to the following spin Hamiltonian:

$$\hat{H} = -2J_1[\hat{S}_{rad}\cdot(\hat{S}_{M1}+\hat{S}_{M2})] - 2J_2(\hat{S}_{M1}\cdot\hat{S}_{M2}) + D\left[\sum_{M=1}^{2}\left(\hat{S}_{z,M}^2 - \frac{1}{3}\hat{S}_M^2\right)\right] + \mu_B g_M(\hat{S}_{M1}+\hat{S}_{M2})H + \mu_B g_{rad}\hat{S}_{rad}H$$

Where $J_1$ and $J_2$ are the $M^{II}$-radical and the $M^{II}$-$M^{II}$ exchange coupling constants, with $M^{II}$ = Fe and Co, for **1** and **2**, respectively. The third term represents the $M^{II}$ axial zero-field splitting, *D*, while the last two terms account for the Zeeman interactions, including both the $M^{II}$ and the radical contributions. The best fit gave the following parameters: $J_1$ = - 218.8 $cm^{-1}$, $J_2$ = + 1.0 $cm^{-1}$, $D_{Fe}$ = + 9.85, and $g_{Fe}$ = 2.09 for **1**, and $J_1$ = - 213.1 $cm^{-1}$, $J_2$ = + 2.5 $cm^{-1}$, $D_{Co}$ = + 18.04, and $g_{Co}$ = 2.50 for **2**.

The fitting results reveal weak ferromagnetic $M^{II}$-$M^{II}$ coupling and strong antiferromagnetic $M^{II}$-radical exchange interactions. Note that the value of the $Co^{II}$-dpq radical exchange in **2** is lower that the values obtained using phenazine (~-500 $cm^{-1}$),[14] tetraazalene (-396 $cm^{-1}$)[15] or hexaazatrinaphthylene-based (-290 $cm^{-1}$)[16] radicals but considerably higher than those reported using nindigo-based (-137 $cm^{-1}$),[17] bptz (-67.5 $cm^{-1}$)[8d], oxazolidine nitroxide (-63.5 $cm^{-1}$)[18], bmtz (-62.5 $cm^{-1}$)[8a] or chloranilate (-52 $cm^{-1}$)[19] radicals. The $Fe^{II}$-dpq radical coupling is larger than that observed for the tetraoxolene (-57 to -65 $cm^{-1}$)[20] or chloranilate (+19 $cm^{-1}$)[19] radicals but smaller that than that reported for the tetraazalene (> 900 $cm^{-1}$)[7] or oxazolidine nitroxide (-315 $cm^{-1}$)[18] radicals. The large and positive *D* and *g* > 2 values obtained for the $Fe^{II}$ and $Co^{II}$ compounds are in good agreement with values reported for other tetrahedral $Fe^{II}$ and $Co^{II}$ ions.[21] Attempts to fit the data in the 2.0-300 K region were unsuccessful due to the precipitous decline below 10 K. The inclusion of an intermolecular z*J* interaction (including and excluding $J_2$) did not improve the fitting and gave unreasonable values for $J_1$, $J_2$, *D*, and *g* parameters.

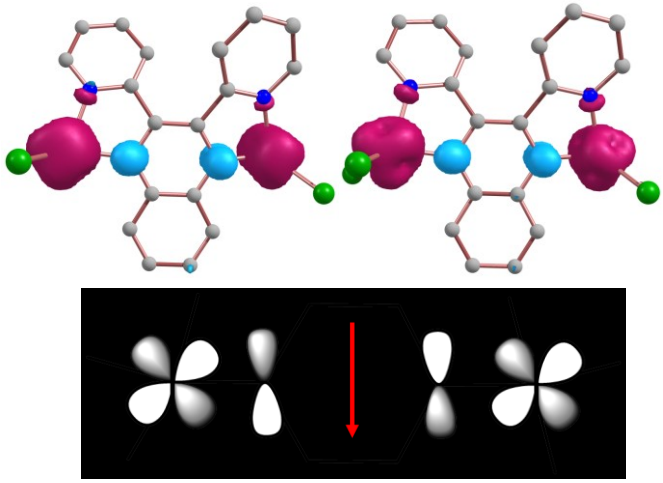

**Figure 4.** DFT computed spin density plots for (top left) **1** and (top right) **2**. The red and blue isodensity surfaces (0.0043 $e^-$ $bohr^{-3}$) indicate positive and negative spin phases, respectively. (bottom) Molecular Orbital (MO) diagram showing the antiferromagnetic interactions between radical and $Fe^{II}$/$Co^{II}$ centers in **1** and **2**.

Using Density Functional Theory (DFT) and *ab initio* CASSCF (Complete Active Space Self-Consistent Field) calculations, the magnetic exchange interactions (*J*), and *g* and *D* parameters were computed (See Computational details in SI). Density Functional Theory (DFT) calculations were performed by using B3LYP functionals[22] to compute the neighboring exchange interaction between metal-radical centers and the next neighboring exchange interaction between metal centers in both complexes (See Computational details in SI). The $J_{M^{II}\text{-rad}}$ values were calculated to be -224.3 $cm^{-1}$ and -242.4 $cm^{-1}$ and the $J_{M^{II}\text{-}M^{II}}$ values were computed to be +2.1 $cm^{-1}$ and +2.4 $cm^{-1}$ for **1** and **2**, respectively (Tables S4 and S5). The calculations reproduce the sign of the experimentally determined magnetic coupling values very well, but the magnitude is slightly overestimated. DFT computed *J* values confirm spin ground states of S = 7/2 and S = 5/2 for **1** and **2**, respectively which arise when the $M^{II}$ ions have spin-up configurations and the dpq radical has a spin-down configuration (Figure 4, top). In both the complexes, the unpaired electron from the $t_2$ magnetic orbital of $M^{II}$ ion overlaps with the π* orbital of the dpq radical (Figure 4, bottom) which leads to the strong antiferromagnetic coupling between them.[8d]

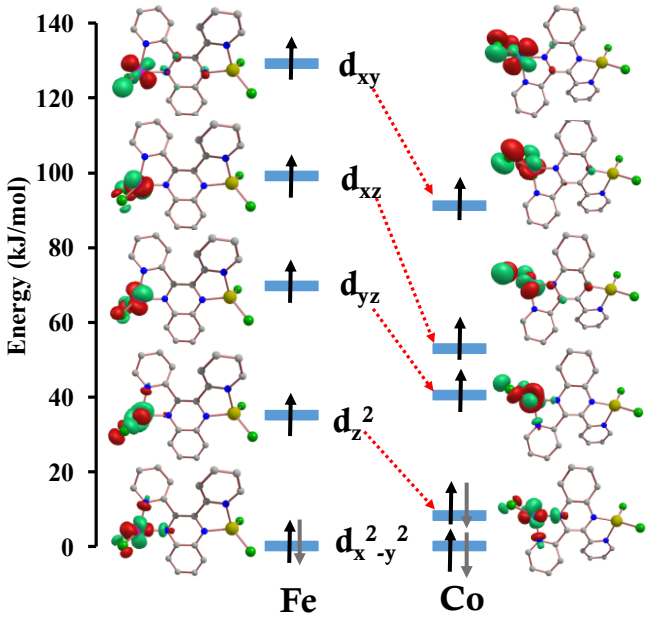


**Figure 5.** *Ab initio* computed d-orbital ordering for $Fe^{II}$ and $Co^{II}$ ions in **1** and **2**, respectively.

To further understand the observed magnetic behavior in **1** and **2**, the *g* and *D* parameters of the $Fe^{II}$ and a $Co^{II}$ ions were computed using *ab initio* CASSCF calculations. The CASSCF calculations yielded *g* values of 2.10 and 2.38, *D* values of 8.2 $cm^{-1}$ and 18.7 $cm^{-1}$, and E/D values of 0.17 and 0.08 for an $Fe^{II}$ and a $Co^{II}$ ion in **1** and **2**, respectively. The computed *g* and *D* values are in good agreement with the experimentally

determined parameters and are in the range of values expected for anisotropic $Fe^{II}$ and $Co^{II}$ ions.[8d, 15, 19] Using the eigenvalue plots, the calculated sign and magnitude of the *D* value of a $Fe^{II}/Co^{II}$ ion in **1** and **2** were rationalized (see Figure 5). The orbital splitting pattern indicates a spin-allowed excitation of a β-electron between the orbitals with different $|\pm m_l|$ levels ($d_{x^2-y^2} \rightarrow d_{z^2}$ for the $Fe^{II}$ ion and $d_{z^2} \rightarrow d_{yz}$ for the $Co^{II}$ ion), which leads to a positive *D* value for these ions.[23] The major positive contribution to the *D* value is from the first four quintet and quartet excited states for the $Fe^{II}$ and the $Co^{II}$ ions, respectively (Table S6). For the $Co^{II}$ ion in **2**, the energy gap between the ground and the first excited state is large (1853.8 $cm^{-1}$) compared to the $Fe^{II}$ ion in **1** (1707.2 $cm^{-1}$). Thus, the positive *D* contribution is significantly larger for the $Co^{II}$ ion compared to $Fe^{II}$ ion due to this very low-lying first excited state, whereas the other excited states marginally contribute to the total positive *D* value.

In summary, the new family of compounds $(Cp^*_2Co)[M_2Cl_4(dpq)]$ (M = Fe, Co, Zn) is reported. The presence of the ligand-centered radical was confirmed by X-ray crystallography, SQUID magnetometry, and EPR spectroscopy. In these complexes, which are the first compassed based on the radical form of the dpq ligand, the metal ions are four-coordinate with tetrahedral geometries. Both complexes **1** and **2** exhibit strong antiferromagnetic metal radical coupling, as evidenced by the large negative coupling constants. DFT and *ab initio* computed spin-Hamiltonian parameters are in good agreement with the experimentally determined values and they nicely reproduce the magnetic susceptibility data. Further studies involving the coordination geometry of the 3d- or 4f-metal ions with this and other structurally similar ligands will be reported in due course.

We gratefully acknowledge support for this work by the National Science Foundation (CHE-1808779) and the Robert A. Welch Foundation (Grant A-1449). The SQUID magnetometer was purchased with funds provided by the Texas A&M University Vice President of Research. We would like to thank the HPRC at Texas A&M University for providing computing resources.

## Conflicts of interest

There are no conflicts to declare.

## Notes and references

1. (a) G. Christou, D. Gatteschi, D. N. Hendrickson and R. Sessoli, *MRS Bulletin*, 2000, **25**, 66-71; bR. Bagai and G. Christou, *Chem. Soc. Rev.*, 2009, **38**, 1011-1026.
2. R. Sessoli, D. Gatteschi, A. Caneschi and M. A. Novak, *Nature*, 1993, **365**, 141.
3. L. Bogani and W. Wernsdorfer, *Nat. Mat.*, 2008, **7**, 179.
4. E. Moreno-Pineda, C. Godfrin, F. Balestro, W. Wernsdorfer and M. Ruben, *Chem. Soc. Rev.*, 2018, **47**, 501-513.
5. S. Demir, I.-R. Jeon, J. R. Long and T. D. Harris, *Coord. Chem. Rev.*, 2015, **289-290**, 149-176.
6. J. D. Rinehart, M. Fang, W. J. Evans and J. R. Long, *J. Am. Chem. Soc.*, 2011, **133**, 14236-14239.
7. I.-R. Jeon, J. G. Park, D. J. Xiao and T. D. Harris, *J. Am. Chem. Soc.*, 2013, **135**, 16845-16848.
8. (a) T. J. Woods, M. F. Ballesteros-Rivas, S. M. Ostrovsky, A. V. Palii, O. S. Reu, S. I. Klokishner and K. R. Dunbar, *Chem. Eur. J.*, 2015, **21**, 10302-10305; (b) T. J. Woods, H. D. Stout, B. S. Dolinar, K. R. Vignesh, M. F. Ballesteros-Rivas, C. Achim and K. R. Dunbar, *Inorg. Chem.*, 2017, **56**, 12094-12097; (c) B. S. Dolinar, S. Gomez-Coca, D. I. Alexandropoulos and K. R. Dunbar, *Chem. Commun.*, 2017, **53**, 2283-2286; (d) D. I. Alexandropoulos, B. S. Dolinar, K. R. Vignesh and K. R. Dunbar, *J. Am. Chem. Soc.*, 2017, **139**, 11040-11043; (e) B. S. Dolinar, D. I. Alexandropoulos, K. R. Vignesh, T. A. James and K. R. Dunbar, *J. Am. Chem. Soc.*, 2018, **140**, 908-911.
9. (a) K. C. Gordon, A. H. R. Al-Obaidi, P. M. Jayaweera, J. J. McGarvey, J. F. Malone and S. E. J. Bell, *J. Chem. Soc., Dalton Trans.*, 1996, 1591-1596; (b) A. Hasheminasab, J. T. Engle, J. Bass, R. S. Herrick and C. J. Ziegler, *Eur. J. Inorg. Chem.*, 2014, **2014**, 2643-2652; (c) P. Alborés, C. Plenk and E. Rentschler, *Inorg. Chem.*, 2012, **51**, 8373-8384; dB. Floris, M. P. Donzello, C. Ercolani and E. Viola, *Coord. Chem. Rev.*, 2017, **347**, 115-140.
10. P. Richardson, D. I. Alexandropoulos, L. Cunha-Silva, G. Lorusso, M. Evangelisti, J. Tang and T. C. Stamatatos, *Inorg. Chem. Front.*, 2015, **2**, 945-948.
11. (a) W. Liu and H. H. Thorp, *Inorg. Chem.*, 1993, **32**, 4102-4105; (b) I. D. Brown and D. Altermatt, *Acta Crys. Sec. B*, 1985, **41**, 244-247.
12. P.-H. Lin, N. C. Smythe, S. I. Gorelsky, S. Maguire, N. J. Henson, I. Korobkov, B. L. Scott, J. C. Gordon, R. T. Baker and M. Murugesu, *J. Am. Chem. Soc.*, 2011, **133**, 15806-15809.
13. N. F. Chilton, R. P. Anderson, L. D. Turner, A. Soncini and K. S. Murray, *J. Comp. Chem.*, 2013, **34**, 1164-1175.
14. X. Ma, E. A. Suturina, S. De, P. Négrier, M. Rouzières, R. Clérac and P. Dechambenoit, *Angew. Chem.Int.Ed*, 2018, **57**, 7841-7845.
15. J. A. DeGayner, I.-R. Jeon and T. D. Harris, *Chem. Sci.*, 2015, **6**, 6639-6648.
16. J. O. Moilanen, N. F. Chilton, B. M. Day, T. Pugh and R. A. Layfield, *Angew. Chem. Int. Ed.*, 2016, **55**, 5521-5525.
17. S. Fortier, J. J. Le Roy, C.-H. Chen, V. Vieru, M. Murugesu, L. F. Chibotaru, D. J. Mindiola and K. G. Caulton, *J. Am. Chem. Soc.*, 2013, **135**, 14670-14678.
18. (a) I. A. Gass, C. J. Gartshore, D. W. Lupton, B. Moubaraki, A. Nafady, A. M. Bond, J. F. Boas, J. D. Cashion, C. Milsmann, K. Wieghardt and K. S. Murray, *Inorg. Chem.*, 2011, **50**, 3052-3064; (b) I. A. Gass, S. Tewary, A. Nafady, N. F. Chilton, C. J. Gartshore, M. Asadi, D. W. Lupton, B. Moubaraki, A. M. Bond, J. F. Boas, S.-X. Guo, G. Rajaraman and K. S. Murray, *Inorg. Chem.*, 2013, **52**, 7557-7572; (c) I. A. Gass, S. Tewary, G. Rajaraman, M. Asadi, D. W. Lupton, B. Moubaraki, G. Chastanet, J.-F. Létard and K. S. Murray, *Inorg. Chem.*, 2014, **53**, 5055-5066.
19. K. S. Min, A. G. DiPasquale, J. A. Golen, A. L. Rheingold and J. S. Miller, *J. Am. Chem. Soc.*, 2007, **129**, 2360-2368.
20. A. E. Thorarinsdottir, R. Bjornsson and T. D. Harris, *Inorg. Chem.*, 2020, **59**, 4634-4649.
21. (a) M. Murrie, *Chem. Soc. Rev.*, 2010, **39**, 1986-1995; (b) J. M. Frost, K. L. M. Harriman and M. Murugesu, *Chem. Sci.*, 2016, **7**, 2470-2491.
22. A. D. Becke, *J. Chem. Phys.*, 1993, **98**, 5648-5652.
23. aS. Gomez-Coca, E. Cremades, N. Aliaga-Alcalde and E. Ruiz, *J. Am. Chem. Soc.*, 2013, **135**, 7010-7018; bT. J. Woods, M. F. Ballesteros-Rivas, S. Gómez-Coca, E. Ruiz and K. R. Dunbar, *J. Am. Chem. Soc.*, 2016, **138**, 16407-16416.